Determination of large-scale mass fluxes from ERA-Interim

Ann'Sophie Tissier[1], Bernard Legras[1]

[1] Laboratoire de Météorologie Dynamique, UPMC/CNRS/ENS/Ecole Polytechnique, Paris, France

GEWEX 29/04/2016

Introduction

Definitions and transport

The tropical tropopause layer and the 380K surface

Key region in the atmosphere :
It controls the transport of air detrained from tropical cumulonimbus clouds and also the composition of the air entering the stratosphere.

Which cloudy regions contribute to the upward mass flux at the 380K surface and in which proportions ?

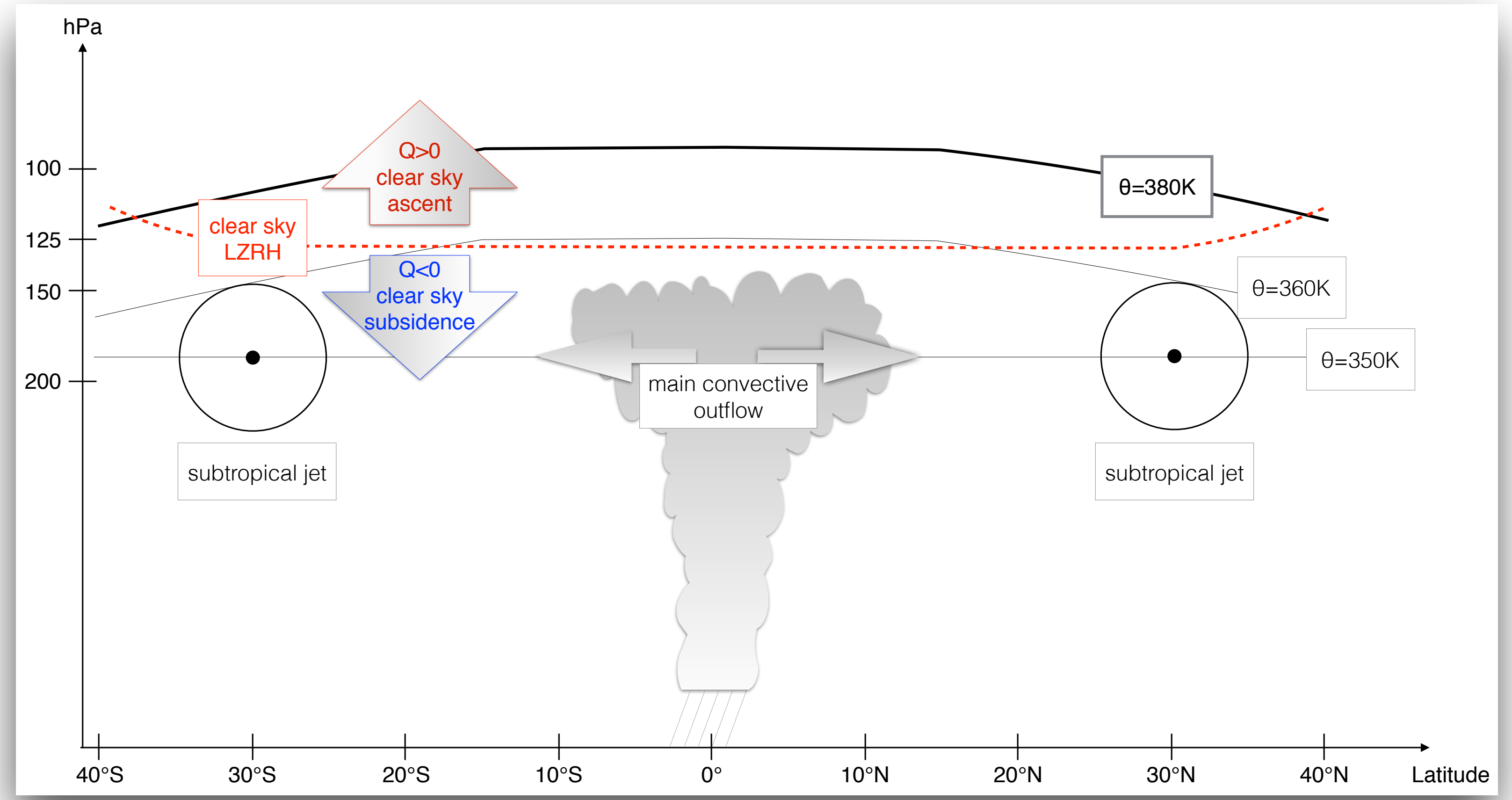

Outline

Introduction

I - Upward mass flux across the 380 K surface : ERA-Interim

II - Backward trajectories : method and convective sources

III - Regional distribution of the mass flux across the 380 K

Summary

I - Upward mass flux across the 380 K surface : ERA-Interim

Method and validation

Monthly upward diabatic mass flux across the 380 K surface, over a specific domain Γ of the sphere :

$$M^{\uparrow}_{\mathrm{diab}} = \iint_{\Gamma} \sigma_{380\mathrm{K}} \left\langle \left. \frac{\mathrm{d}\theta}{\mathrm{d}t} \right|_{380\mathrm{K}} \right\rangle \mathrm{d}s$$

with $\sigma_{380\mathrm{K}} = -\frac{1}{g} \left. \frac{\partial P}{\partial \theta} \right|_{380\mathrm{K}}$ and $\left\langle \left. \frac{\mathrm{d}\theta}{\mathrm{d}t} \right|_{380\mathrm{K}} \right\rangle > 0$

I - Upward mass flux across the 380 K surface : ERA-Interim

Method and validation

Monthly upward diabatic mass flux across the 380 K surface, over a specific domain Γ of the sphere :

$$M^{\uparrow}_{\mathrm{diab}} = \iint_{\Gamma} \sigma_{380\mathrm{K}} \left\langle \left. \frac{\mathrm{d}\theta}{\mathrm{d}t} \right|_{380\mathrm{K}} \right\rangle \mathrm{d}s$$

with $\sigma_{380\mathrm{K}} = -\frac{1}{g} \left. \frac{\partial P}{\partial \theta} \right|_{380\mathrm{K}}$ and $\left\langle \left. \frac{\mathrm{d}\theta}{\mathrm{d}t} \right|_{380\mathrm{K}} \right\rangle > 0$

More traditional method, with residual mean circulation, cf. Andrews et al. (1987), the kinematic flux :

$$M_{\mathrm{kine}} = \int \int \left[\frac{p_{380\,\mathrm{K}}}{gH} \left(\overline{w^*} - \frac{1}{a} \left. \frac{\partial z}{\partial \phi} \right|_{380\,\mathrm{K}} \overline{v^*} \right) + \frac{1}{g} \left. \frac{\partial p}{\partial t} \right|_{380\,\mathrm{K}} \right] \mathrm{d}s$$

with $\overline{v^*} = \overline{v} - \frac{1}{p} \frac{\partial}{\partial z} \left(p \frac{\overline{v'\theta'}}{\overline{\theta_z}} \right)$ and $\overline{w^*} = \overline{w} + \frac{1}{a \cos\phi} \frac{\partial}{\partial \phi} \left(\cos\phi \frac{\overline{v'\theta'}}{\overline{\theta_z}} \right)$

Monthly upward ($M^{\uparrow}_{\mathrm{kine}}$) and downward ($M^{\downarrow}_{\mathrm{kine}}$) mass flux : separated according to the sign of the monthly average term under the integral.

I - Upward mass flux across the 380 K surface : ERA-Interim

Method and validation

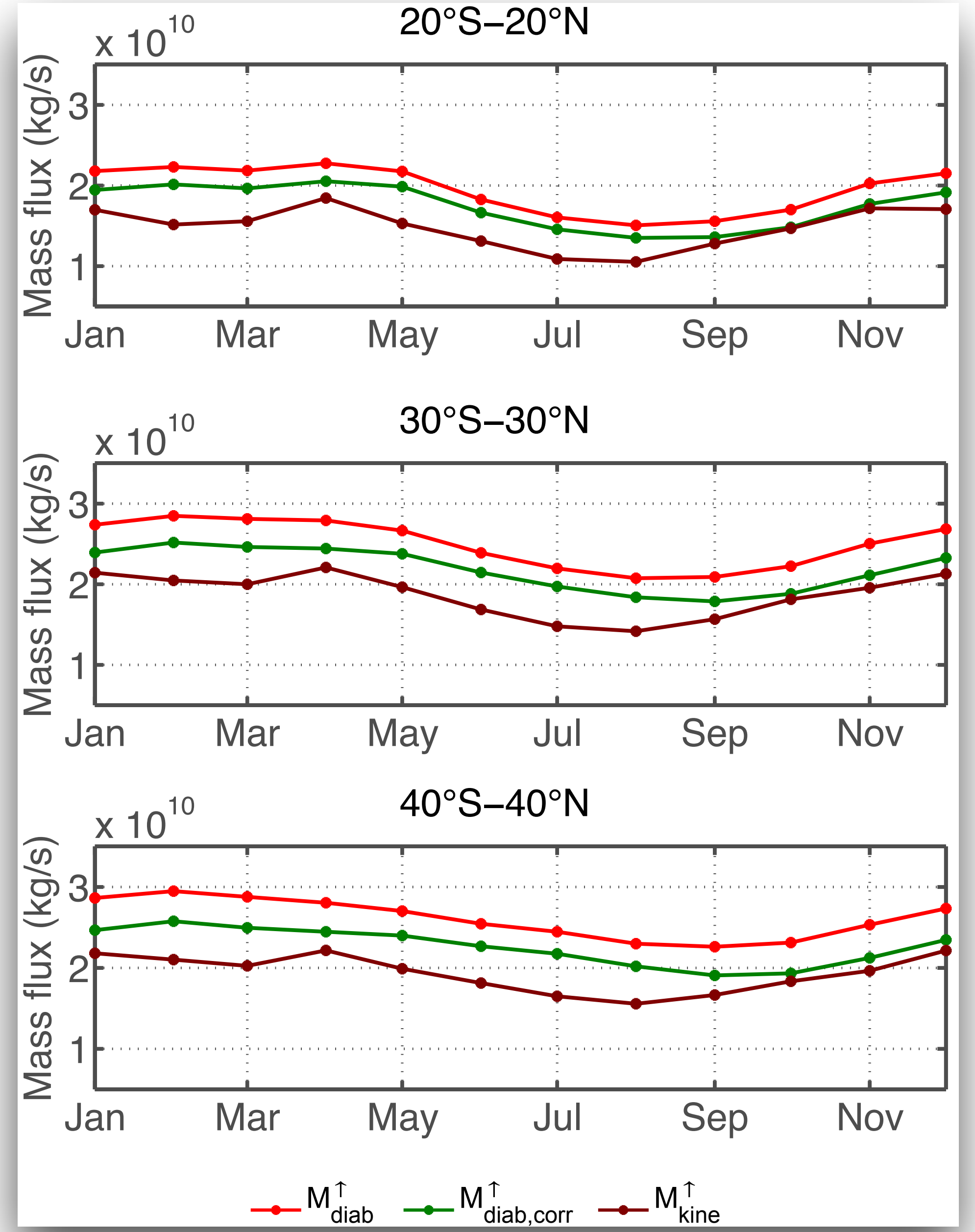

Fig. Annual variations of the monthly upward mass flux at the 380K surface, calculated from ERA-Interim data. Results are averaged over 2005-2008 for each month.

diabatic :

$$M^{\uparrow}_{\text{diab}} = \iint_{\Gamma} \sigma_{380\text{K}} \left\langle \left. \frac{\mathrm{d}\theta}{\mathrm{d}t} \right|_{380\text{K}} \right\rangle \mathrm{d}s$$

kinematic :

$$M^{\uparrow}_{\text{kine}}$$

- Similar summer/winter modulation : Abalos et al., 2012
- But : shift which increases with the size of latitude band

I - Upward mass flux across the 380 K surface : ERA-Interim

Method and validation

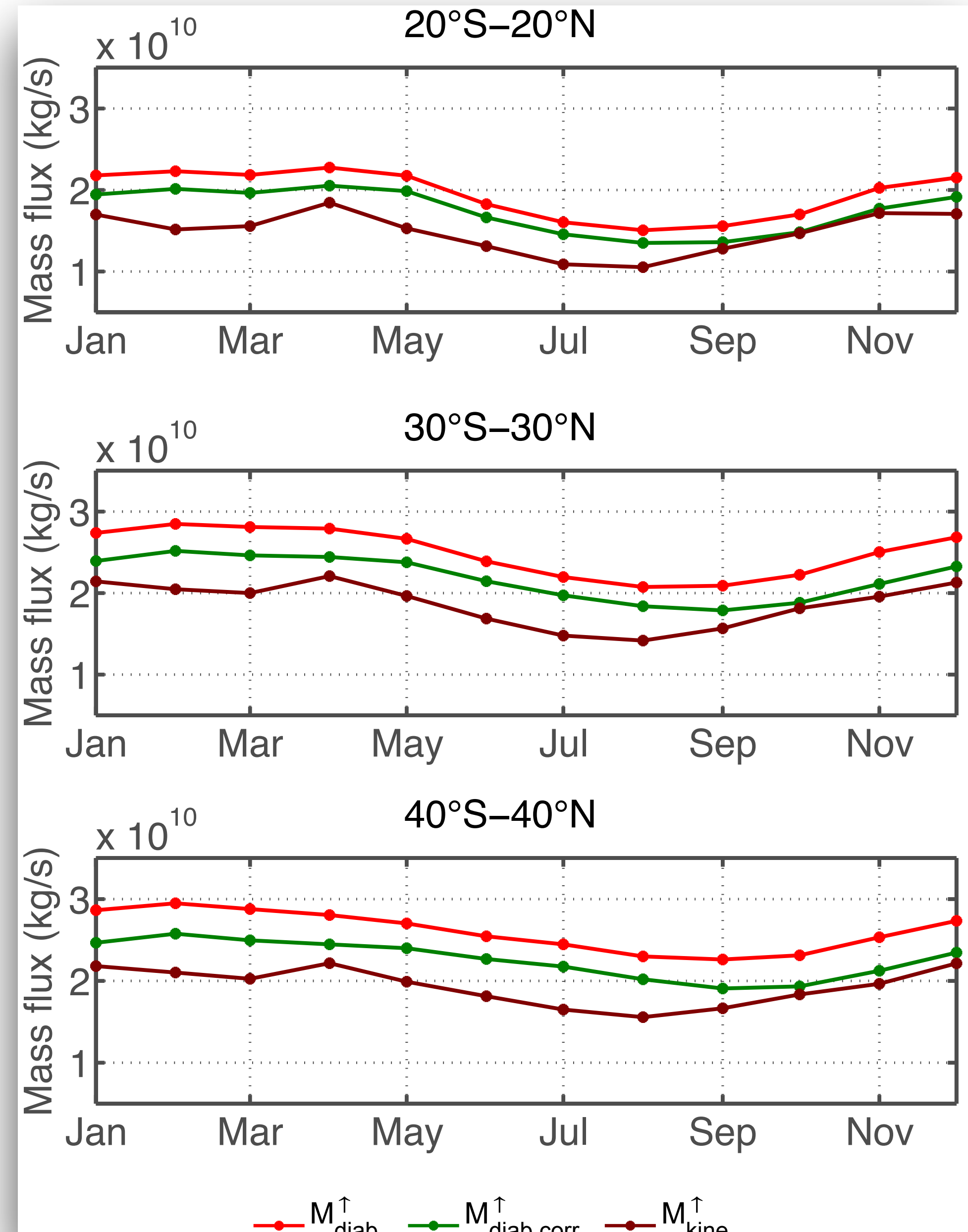

Fig. Annual variations of the monthly upward mass flux at the 380K surface, calculated from ERA-Interim data. Results are averaged over 2005-2008 for each month.

diabatic :

$$M^{\uparrow}_{\mathrm{diab}} = \iint_{\Gamma} \sigma_{380\mathrm{K}} \left\langle \frac{\mathrm{d}\theta}{\mathrm{d}t}\bigg|_{380\mathrm{K}} \right\rangle \mathrm{d}s$$

kinematic :

$$M^{\uparrow}_{\mathrm{kine}}$$

- Similar summer/winter modulation : Abalos et al., 2012
- But : shift which increases with the size of latitude band

Correction diabatic mass flux to satisfy global mass conservation :

$M^{\uparrow}_{\mathrm{diab}}$ —> $M^{\uparrow}_{\mathrm{diab,corr}}$

- But : spatial and temporal distribution of the errors not taken into account

Outline

II - Backward trajectories

Method

Trajectory calculations with TRACZILLA

- TRACZILLA : modified version of FLEXPART ([Stohl and al, 2005], [Pisso and Legras,2008])
- Calculations of backward diabatic trajectories.
- Trajectories are updated every 15 minutes in TRACZILLA.
- Horizontal part of the movement : calculated using wind fields of ERA-Interim.
- Vertical part of the movement : calculated using radiative heating rates of ERA-Interim.

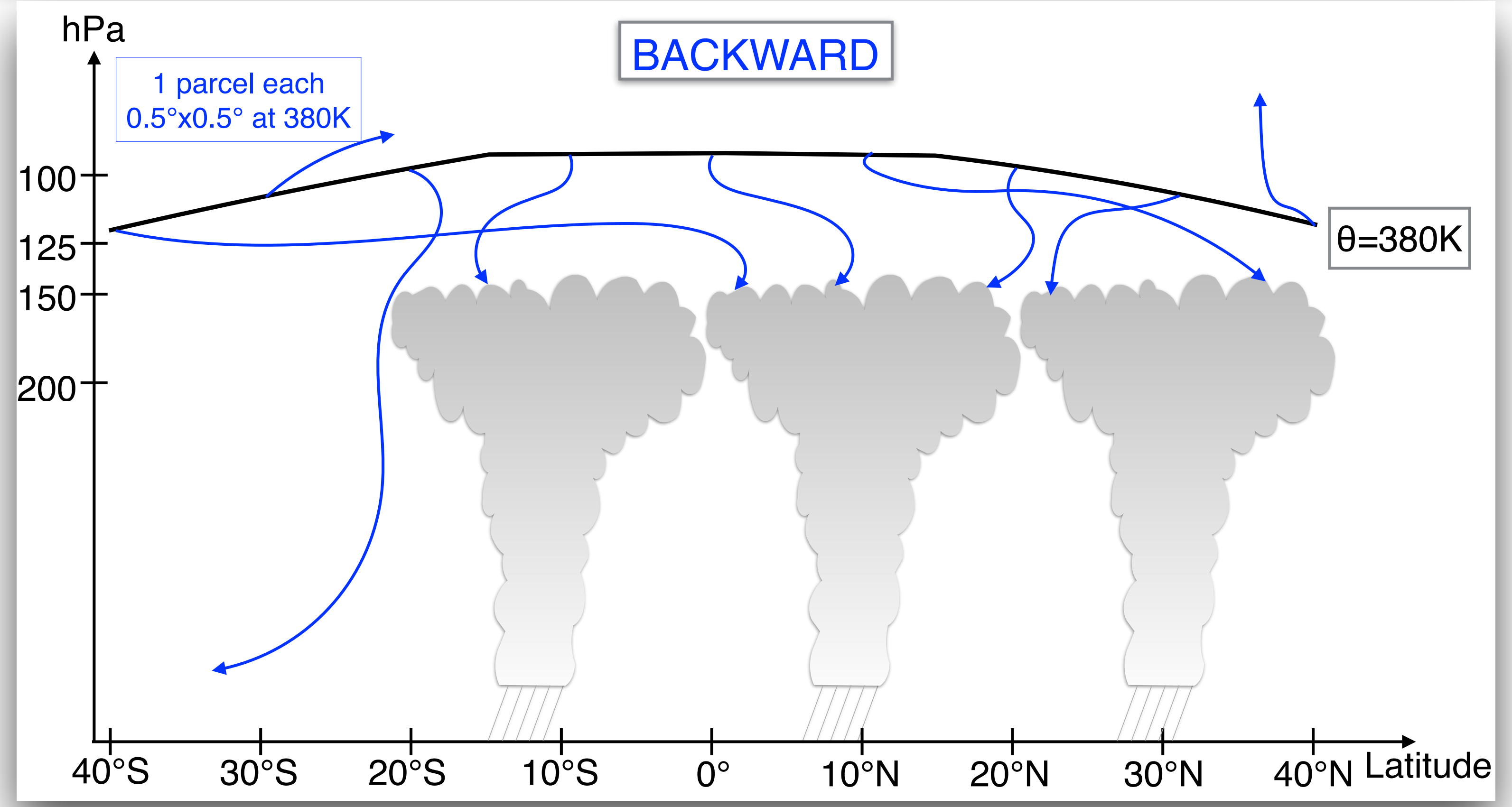

- First intersection in the 3 months.
- Simulation every month in 2005 until 2008.

II - Backward trajectories

Deep convective cloud top determination

CLAUS dataset (Robinson et al., 1999)

- long time series of global thermal infra-red imagery
- provides data of brightness temperature (T_B) every 3 hours
- uniform latitude-longitude grid at high resolution : 1/3°x1/3°

→ 1 pixel with T_B<230K = deep convective cloud top (Young et al. 2013)

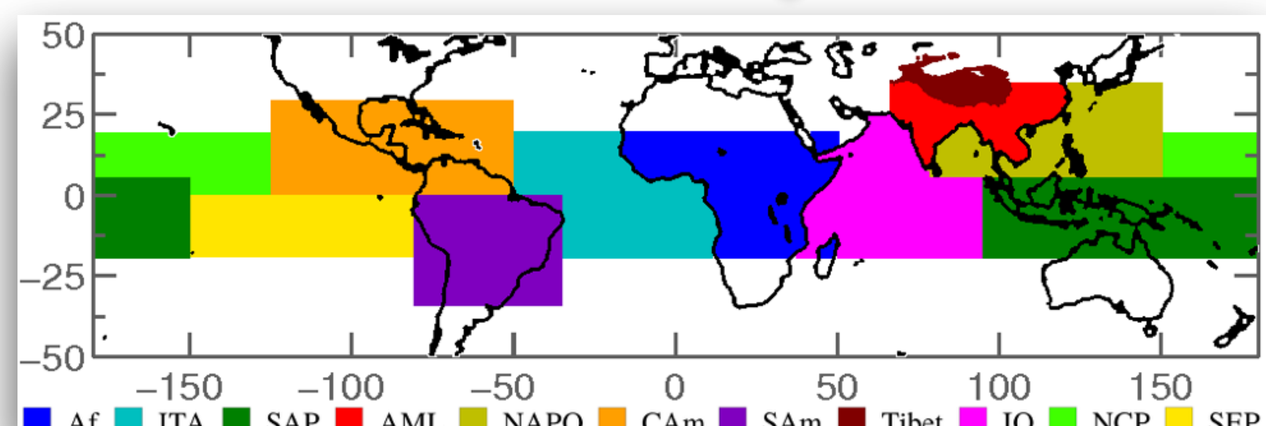

<u>Assumption :</u>

- The temperature at the top of the cloud is equal to the T_B

<u>Underestimation of the cloud top :</u>

- Add a Δz = +1km shift (Sherwood, 2004; Minnis et al. 2008)

II - Backward trajectories

Convective sources of trajectories reaching 380K

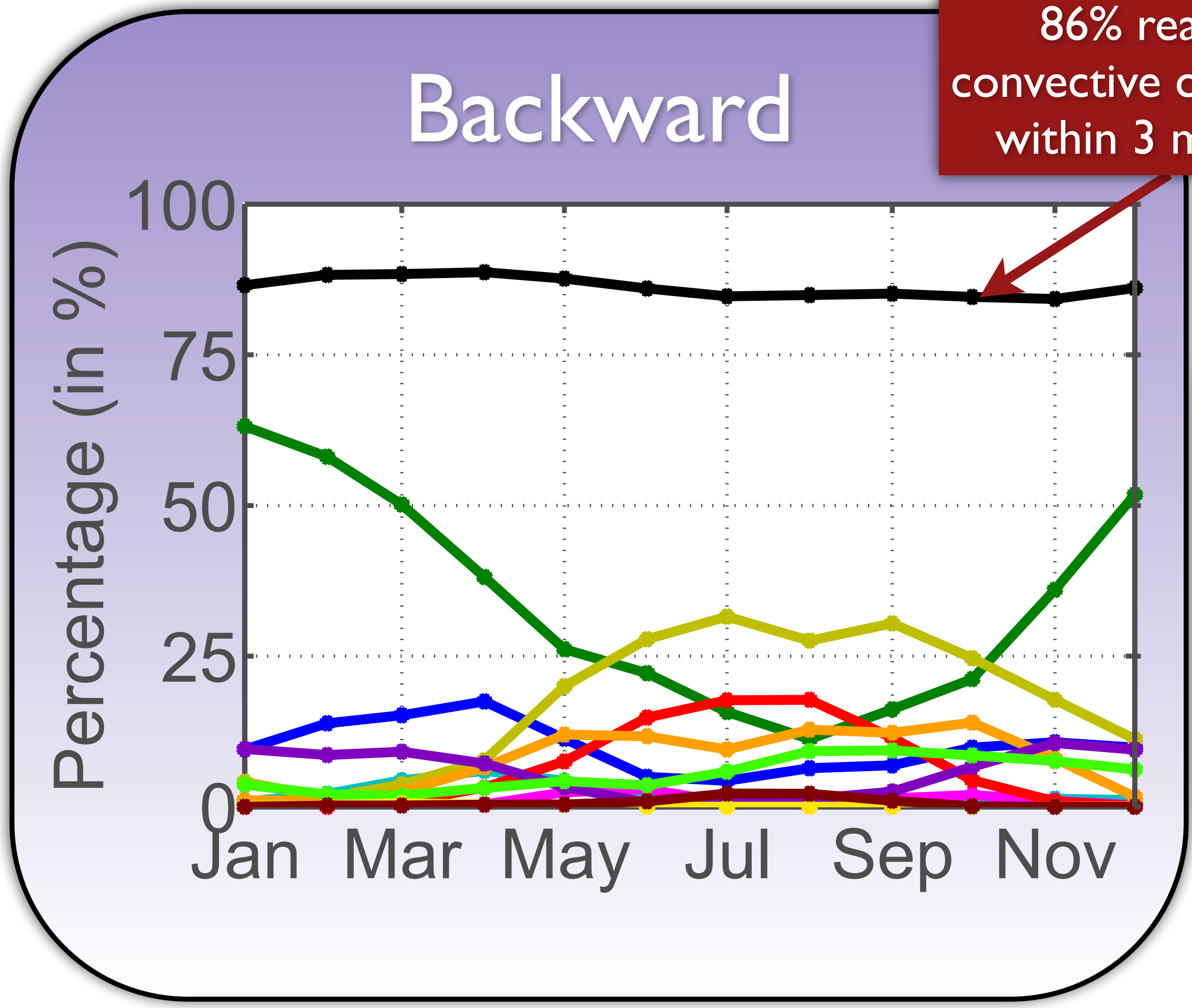

86% reach a convective cloud top within 3 months

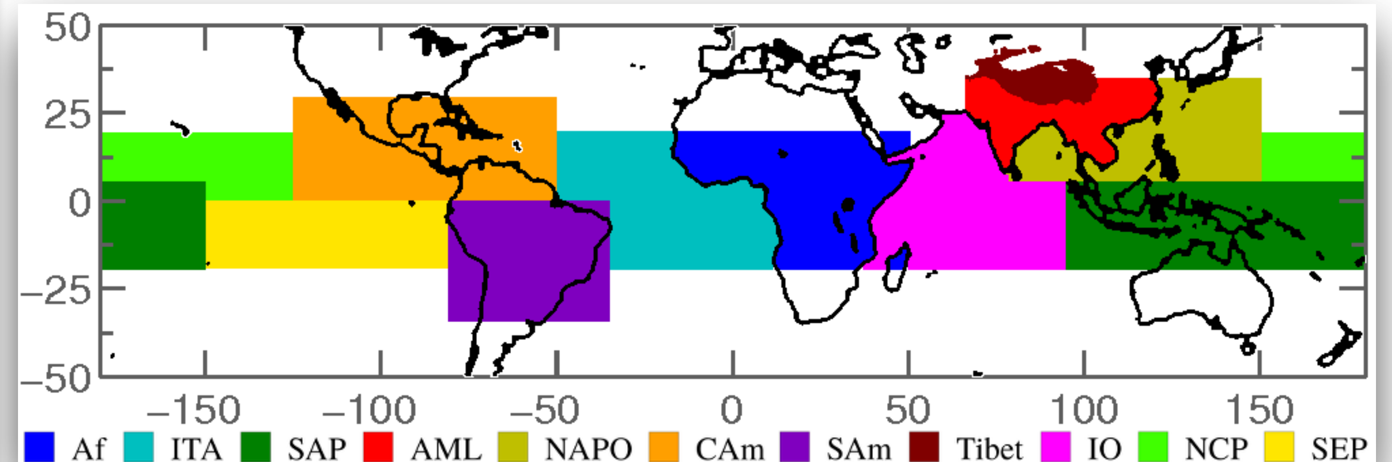

Source distribution among all regions (colored lines) (time : cloud top intersection)

Outline

III - Regional distribution of the mass flux across the 380K surface

Method and validation

Monthly upward diabatic mass flux across the 380 K surface, over a specific domain Γ of the sphere :

$$M^{\uparrow}_{\mathrm{diab}} = \iint_{\Gamma} \sigma_{380\mathrm{K}} \left\langle \left.\frac{\mathrm{d}\theta}{\mathrm{d}t}\right|_{380\mathrm{K}} \right\rangle \mathrm{d}s$$

with $\sigma_{380\mathrm{K}} = -\frac{1}{g} \left.\frac{\partial P}{\partial \theta}\right|_{380\mathrm{K}}$ and $\left\langle \left.\frac{\mathrm{d}\theta}{\mathrm{d}t}\right|_{380\mathrm{K}} \right\rangle > 0$

Monthly upward mass flux, from backward trajectories :

$$M^{\uparrow}_{\mathrm{back}} = \sum_{i \in \Gamma} \sigma_i \frac{\Delta\theta_i}{\Delta t} \delta s_i$$

where δs_i surface of 0.5°x0.5° element associated with the parcel

and the sum $\sum_{i \in \Gamma}$ is applied only where $M^{\uparrow}_{\mathrm{diab}} > 0$

Regional distribution of the upward mass flux

diabatic (uncorrected) :

$$M^{\uparrow}_{\rm diab} = \iint_{\Gamma} \sigma_{380\rm K} \left\langle \left. \frac{{\rm d}\theta}{{\rm d}t} \right|_{380\rm K} \right\rangle {\rm d}s$$

backward trajectories :

$$M^{\uparrow}_{\rm back} = \sum_{i \in \Gamma} \sigma_i \frac{\Delta\theta_i}{\Delta t} \delta s_i$$

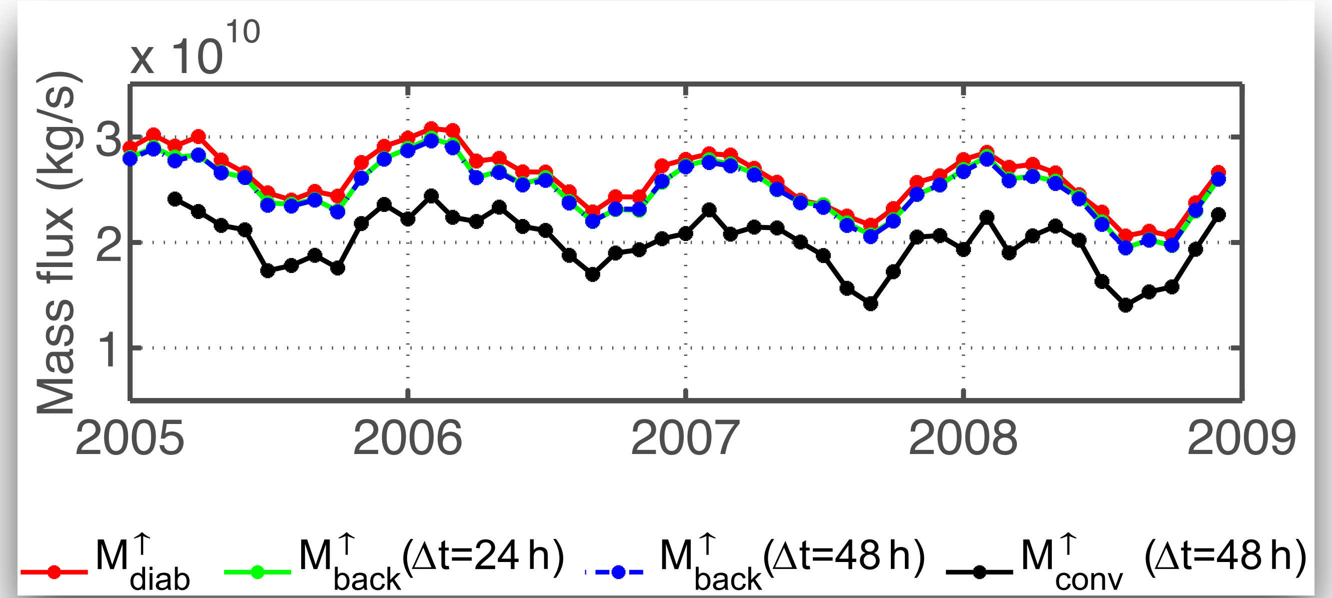

Fig. Upward mass flux at the 380 K surface

- $M^{\uparrow}_{\rm back}$: Δt=24h and Δt=48h cases : similar
- $M^{\uparrow}_{\rm back}$ et $M^{\uparrow}_{\rm diab}$: same order of magnitude

III - Regional distribution of the mass flux across the 380K surface

Regional distribution of the upward mass flux

diabatic (uncorrected) :

$$M^{\uparrow}_{\mathrm{diab}} = \iint_{\Gamma} \sigma_{380\mathrm{K}} \left\langle \left. \frac{\mathrm{d}\theta}{\mathrm{d}t} \right|_{380\mathrm{K}} \right\rangle \mathrm{d}s$$

backward trajectories :

$$M^{\uparrow}_{\mathrm{back}} = \sum_{i \in \Gamma} \sigma_i \frac{\Delta\theta_i}{\Delta t} \delta s_i$$

Convective upward flux :

$$M^{\uparrow}_{\mathrm{conv}}$$

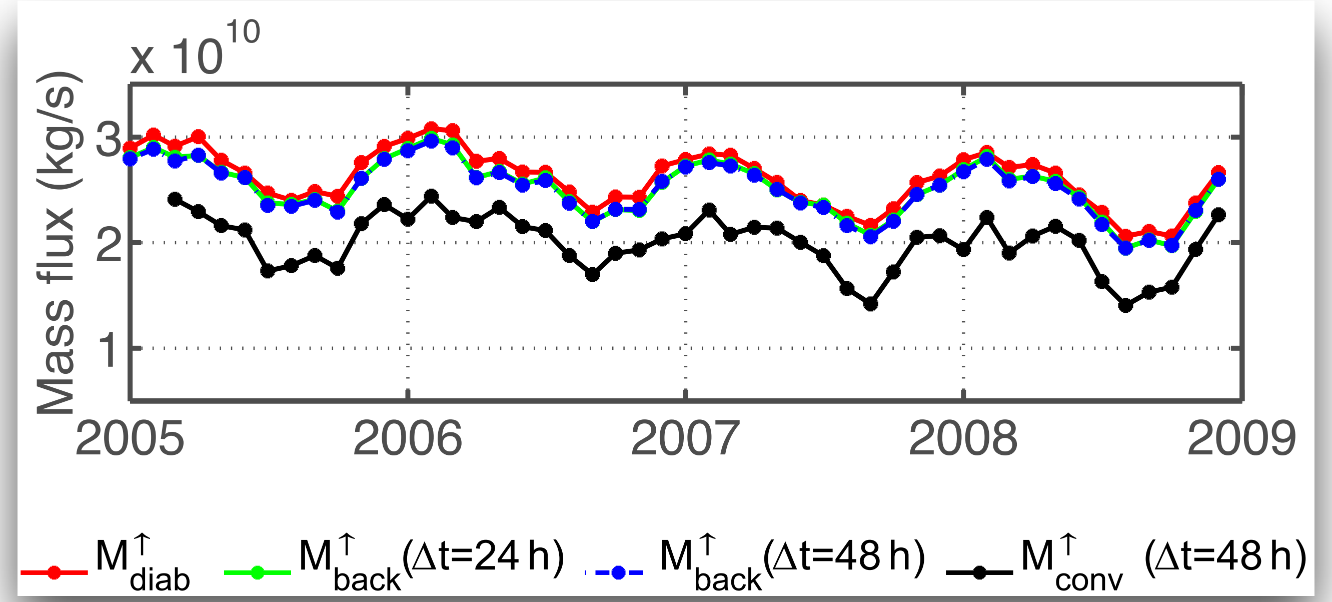

Fig. Upward mass flux at the 380 K surface

- $M^{\uparrow}_{\mathrm{back}}$: Δt=24h and Δt=48h cases : similar
- $M^{\uparrow}_{\mathrm{back}}$ et $M^{\uparrow}_{\mathrm{diab}}$: same order of magnitude

$$100 \times \frac{M^{\uparrow}_{\mathrm{conv}}}{M^{\uparrow}_{\mathrm{back}}}$$

- Mean : 80.0%
- DJF : 80.5%
- JJA : 78.7%

III - Regional distribution of the mass flux across the 380K surface

Regional distribution of the upward mass flux

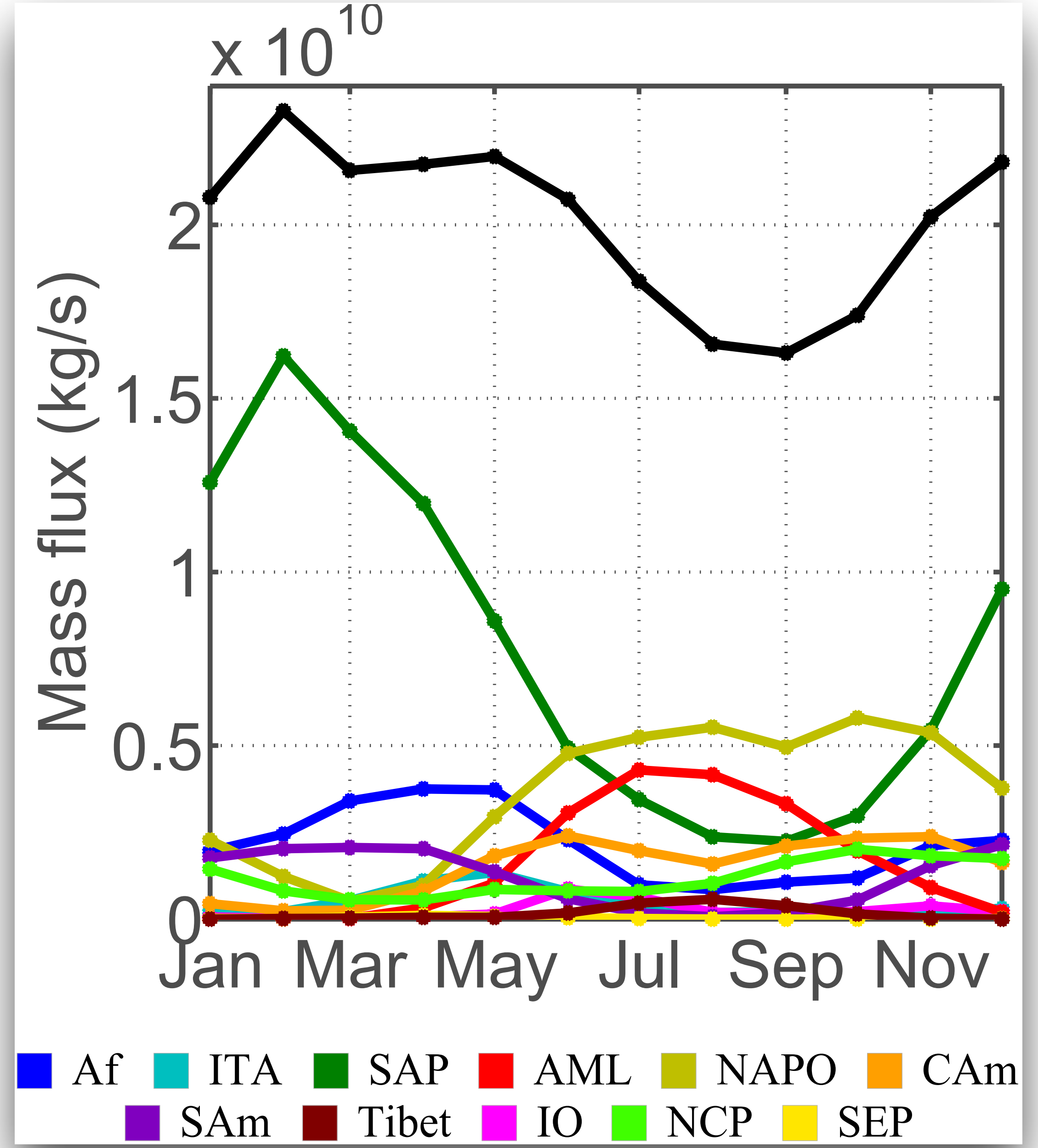

Fig. Mean annual cycles of monthly upward mass fluxes through the 380K surface attributed to each source region.

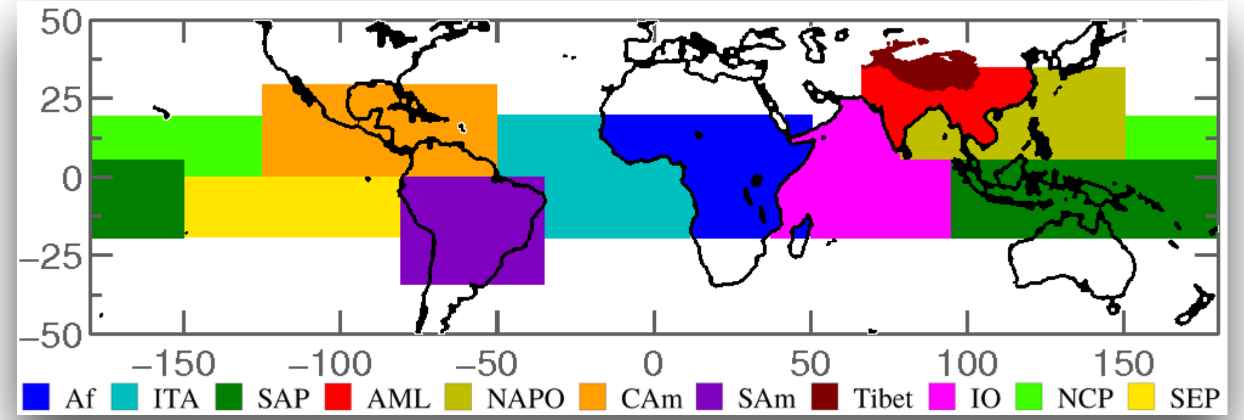

III - Regional distribution of the mass flux across the 380K surface

Regional distribution of the upward mass flux

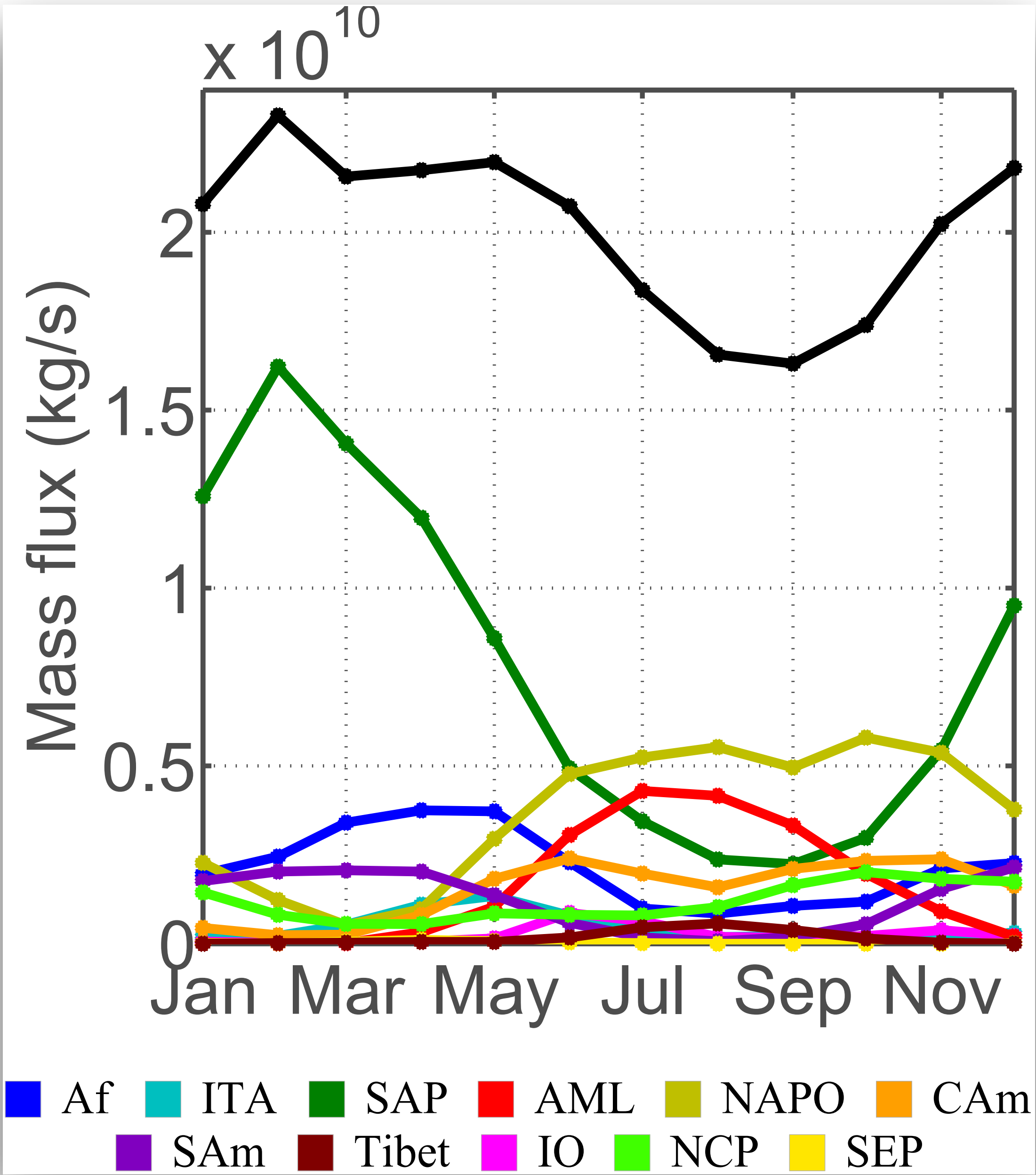

Fig. Mean annual cycles of monthly upward mass fluxes through the 380K surface attributed to each source region.

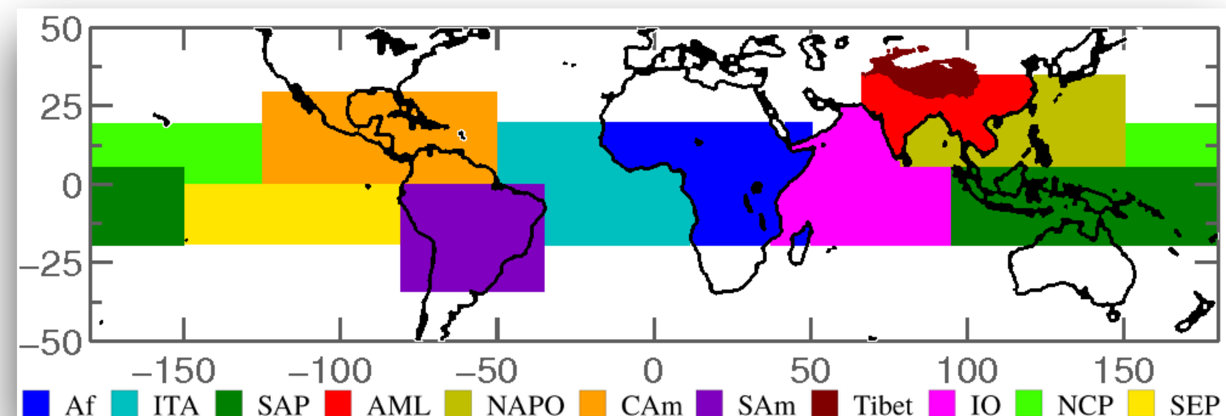

Tab. Distribution of annual mass flux, averaged over 2005-2008, for all regions (in %) :

Af	ITA	SAP	AML	NAPO	CAm	SAm	Tibet	IO	NCP	SEP
10.8	2.4	39.2	8	18	7.5	6	0.8	1.2	5.9	0.2
3rd		1st		2nd						

III - Regional distribution of the mass flux across the 380K surface

Regional distribution of the upward mass flux

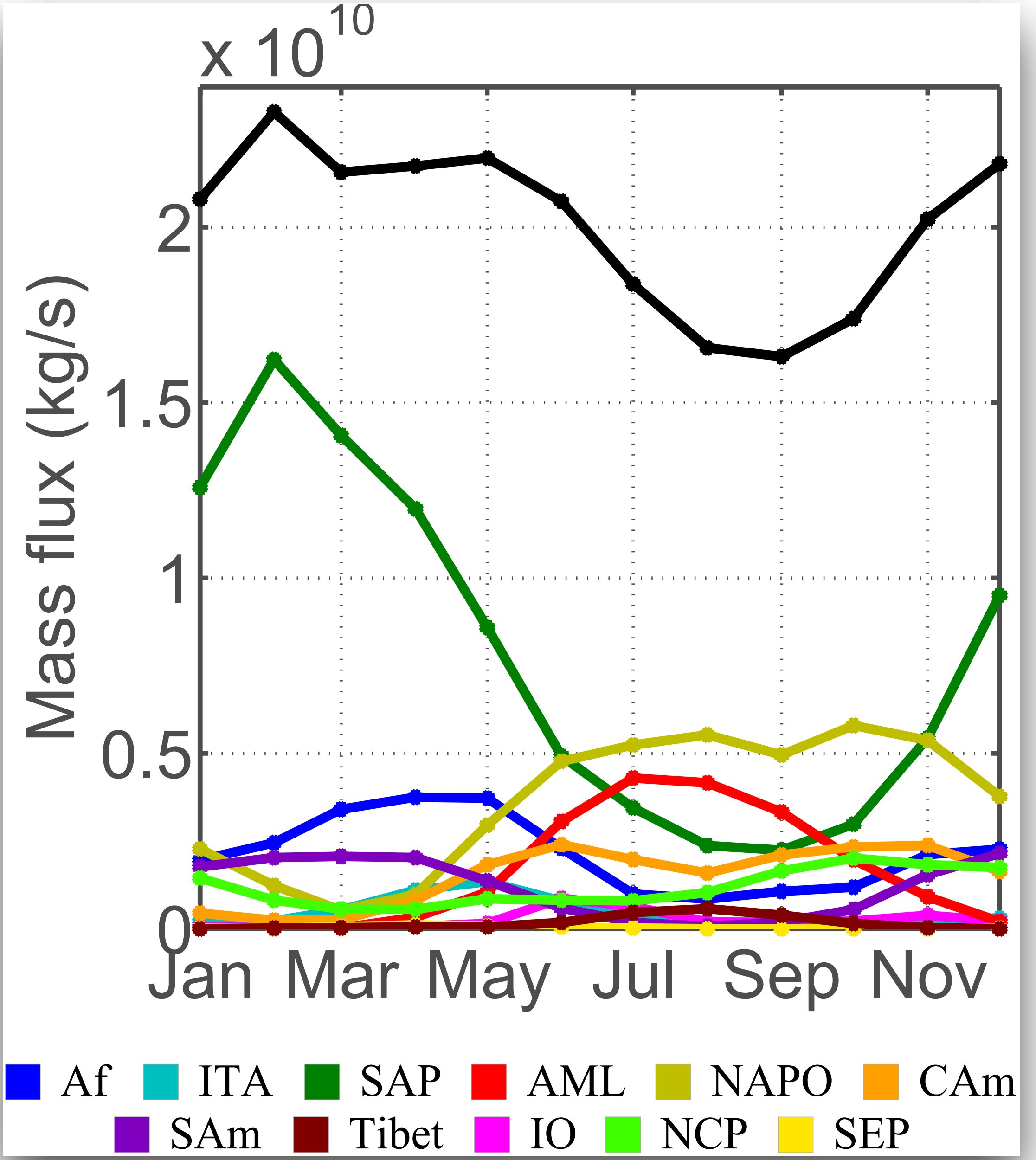

Fig. Mean annual cycles of monthly upward mass fluxes through the 380K surface attributed to each source region.

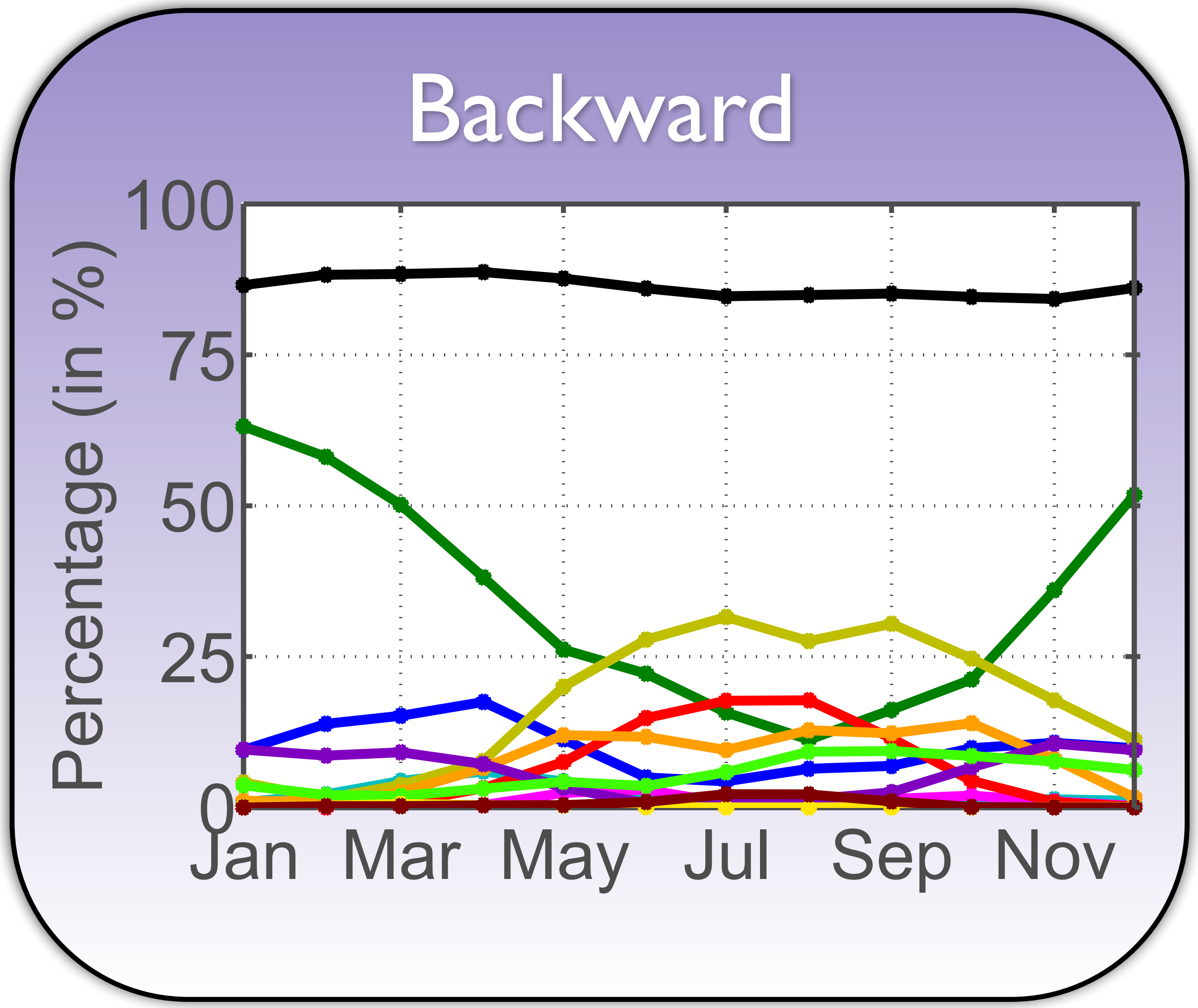

Source distribution among all regions (colored lines)
(time : cloud top intersection)

III - Regional distribution of the mass flux across the 380K surface

Regional distribution of the upward mass flux

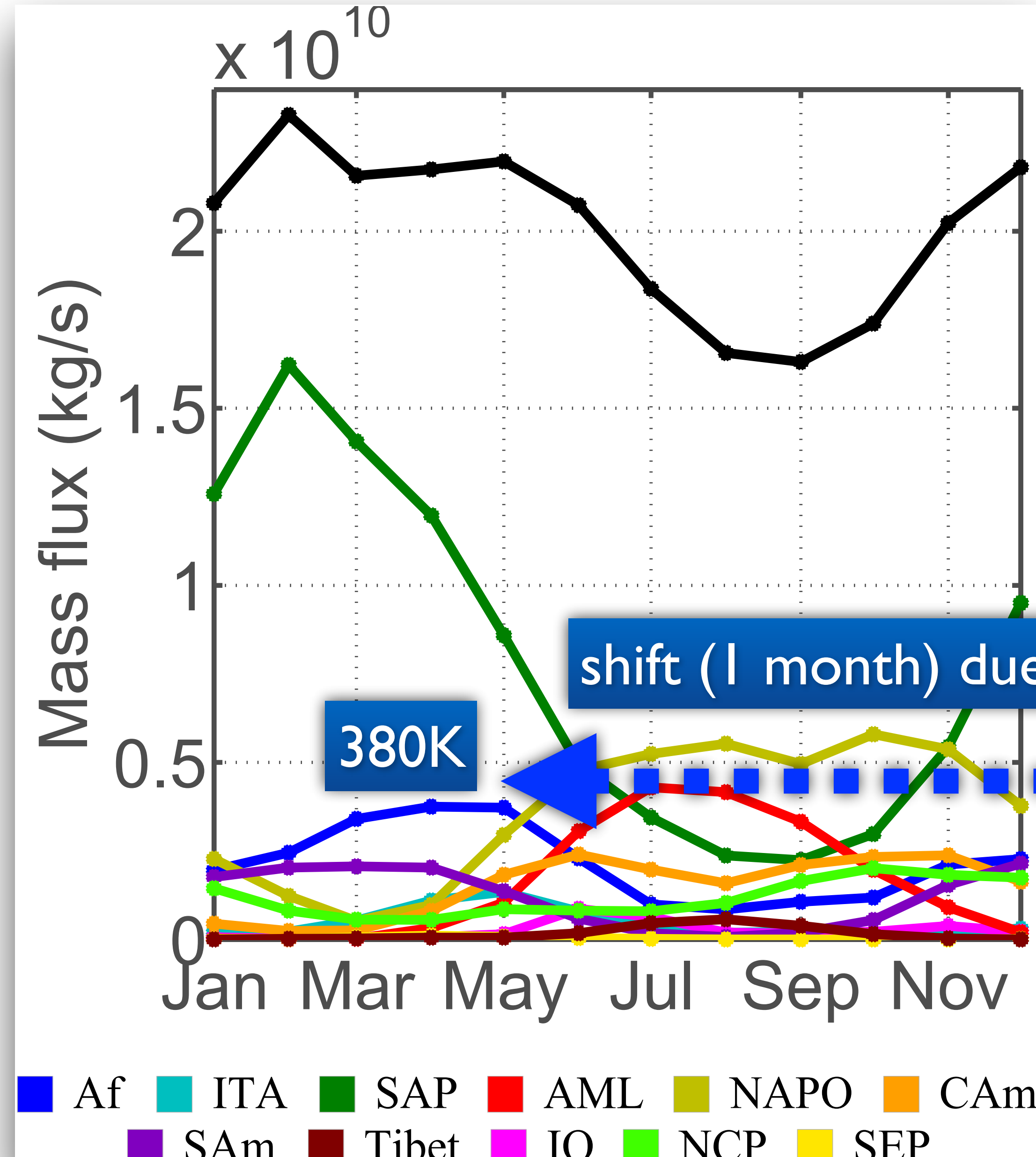

Fig. Mean annual cycles of monthly upward mass fluxes through the 380K surface attributed to each source region.

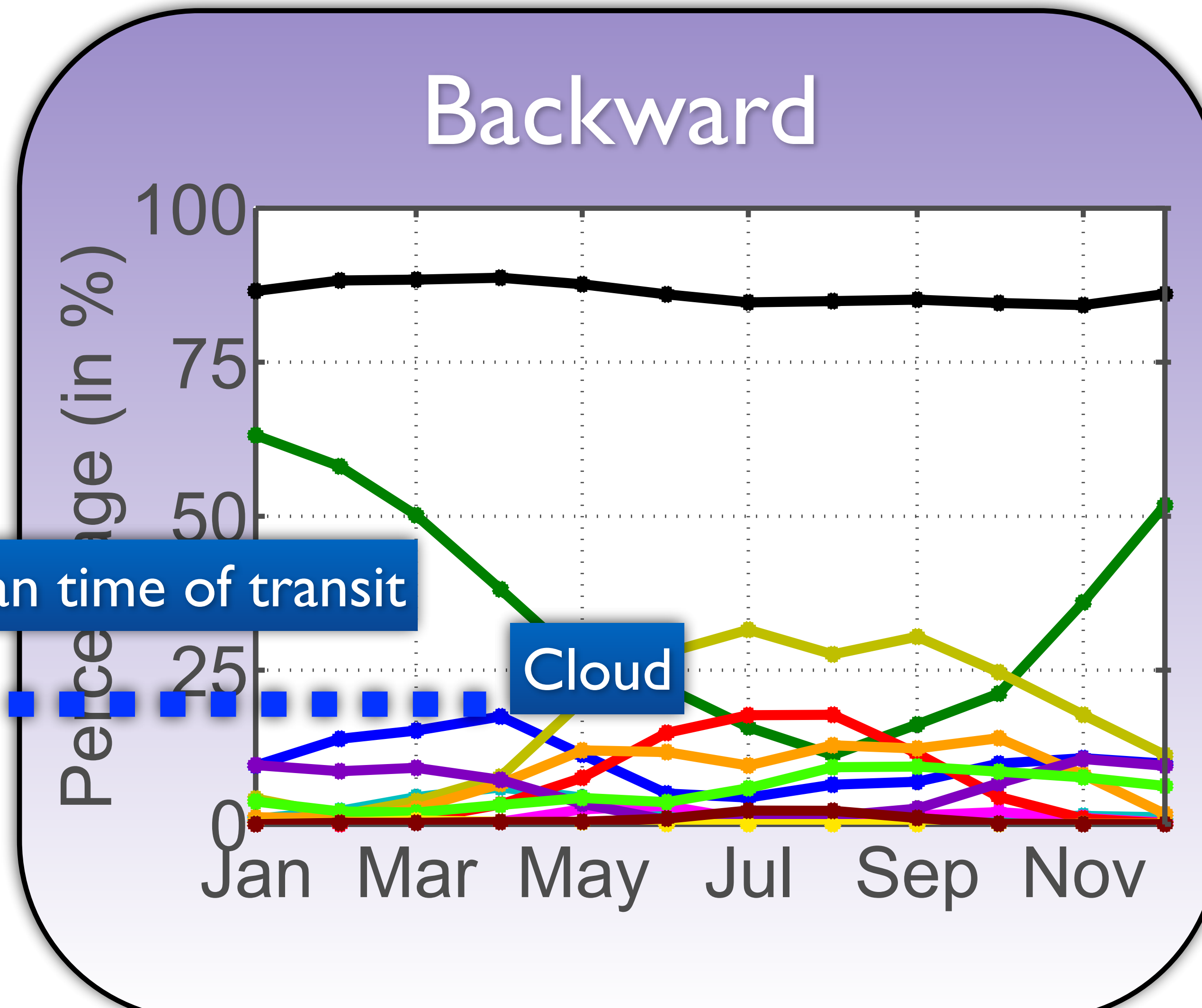

Source distribution among all regions (colored lines) (time : cloud top intersection)

III - Regional distribution of the mass flux across the 380K surface

Regional distribution of the upward mass flux: new Boxes

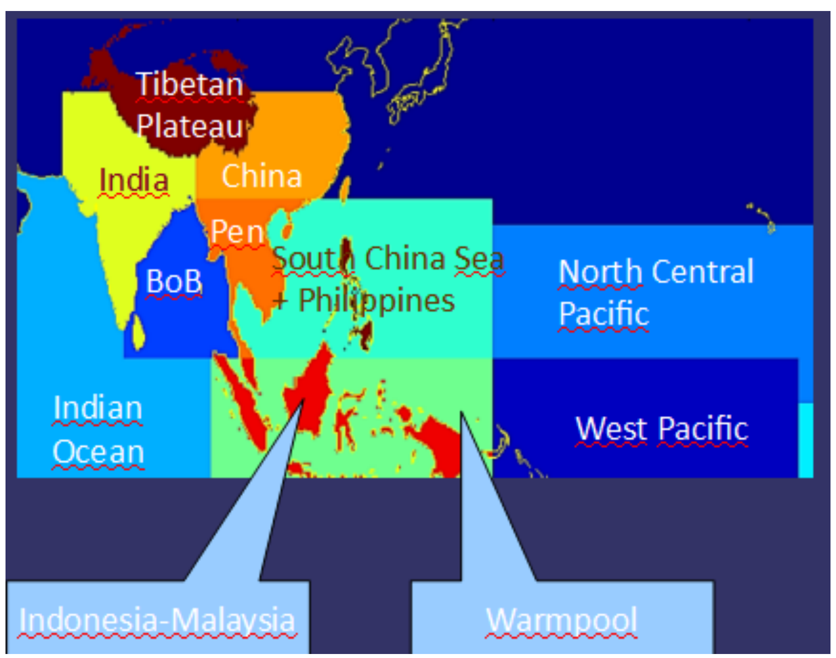

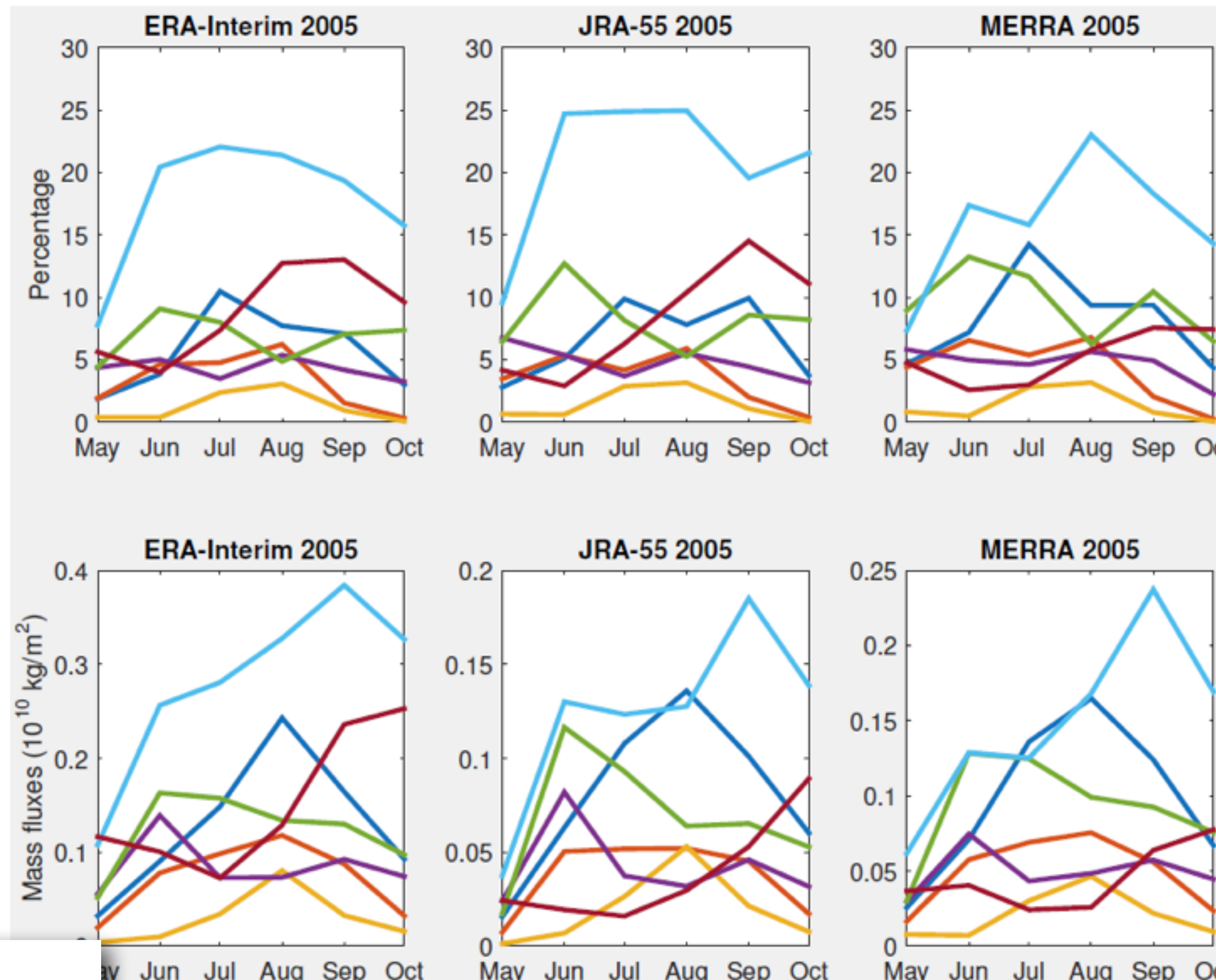

- Distribution of sources in percentages : quite similar among the reanalysis
- Diabatic mass fluxes in ERA-Interim are about twice that of the two other reanalysis

Outline

Introduction

I - Upward mass flux across the 380 K surface : ERA-Interim
II - Backward trajectories : method and convective sources
III - Regional distribution of the mass flux across the 380 K

Summary

Summary

Seasonal cycle of sources is binary with a domination of single South Asia Pacific region (SAP) from November to April, and a more complicated pattern dominated by the region of the Asian monsoon from June to September.

There is a pronounced seasonal cycle of the monthly average upward mass flux across the 380K surface, with a maximum in February and a minimum in September, which is shifted by about a month to the seasonal cycle of sources, due to the mean time of transit of parcels across the TTL.

SAP contribution over the year accounts for 39% of the total $\boxed{M^{\uparrow}_{\mathrm{conv}}}$ while NAPO accounts for 18%.

However : $\boxed{M^{\uparrow}_{\mathrm{conv}}}$ must be taken as an upper bound of the flux of convectively processed air : this air contains convective air detrained from the clouds in the vicinity but is also mixed with environment air.

Determination of large-scale mass fluxes from ERA-Interim

Ann'Sophie Tissier[1], Bernard Legras[1]

[1] Laboratoire de Météorologie Dynamique, UPMC/CNRS/ENS/Ecole Polytechnique, Paris, France

GEWEX 29/04/2016